J Nanostruct 16(3): 3367-3375, Summer 2026

RESEARCH PAPER

Therapeutic Efficacy of Gold Nanoparticles in Ulcerative Colitis Management via NF-κB Pathway Inhibition

Raghad Hasan Nafal *, Ahmed T. Enad, Noor Ali Zayed

Basic Sciences Department, College of Dentistry, Ibn Sina University of Medical and Pharmaceutical Sciences, Baghdad, Iraq

ARTICLE INFO

Article History:
Received 06 April 2026
Accepted 17 May 2026
Published 01 July 2026

Keywords:
Anti-inflammatory
DSS-induced colitis
Gold nanoparticles
Nanomedicine
NF-κB pathway
Ulcerative colitis

ABSTRACT

Ulcerative colitis (UC), a chronic large intestine inflammatory condition, burdens patients and health systems. Many patients benefit from aminosalicylate, corticosteroid, and biological therapy, although side effects, incomplete response, and relapses limit their long-term usage. Due to these restrictions, nanoparticle-based therapy is gaining popularity as a possible alternative. In this study, gold nanoparticles (AuNPs) were synthesised by reducing $HAuCl_4$ with sodium citrate. To assess their therapeutic potential, a dextran sulphate sodium (DSS)-induced UC model in BALB/c mice was UV–Vis, FTIR, XRD, and FESEM were used to characterise the nanoparticles. FTIR showed citrate capping surface functional groups, XRD signals matched metallic gold's face-centered cubic structure, and FESEM showed mainly spherical particles with a mean diameter of 25 nm. Oral AuNPs (5 mg/kg/day) were given to mice for 14 days. The disease activity index, colon length, myeloperoxidase activity, and histological grades improved significantly after treatment. Western blotting and ELISA indicated reductions in TNF-α, IL-1β, and IL-6 levels in colonic tissue compared to the untreated colitic group. AuNPs ameliorate experimental UC by inhibiting the NF-κB signalling pathway, suggesting further research as a supplementary treatment for inflammatory bowel disease.

How to cite this article
Nafal R., Enad A, Zayed N. Therapeutic Efficacy of Gold Nanoparticles in Ulcerative Colitis Management via NF-κB Pathway Inhibition. J Nanostruct, 2026; 16(3):3367-3375. DOI: 10.22052/JNS.2026.03.030

INTRODUCTION

Long-term uncontrolled colonic ulcerative colitis (UC) can lead to bloody diarrhoea, abdominal pain, weight loss, and colorectal cancer [1]. Current studies imply a complicated aetiology involving genetic susceptibility, dysregulated gut microbiota dysbiosis, dysregulated mucosal immunity and environmental stresses [2,3]. The incidence of disease has been on the rise globally, especially in the newly industrialised countries, making it a public health problem [4].

The current therapeutic arsenal includes 5-aminosalicylic acid derivatives, corticosteroids, immunomodulators and anti-TNF antibodies. These drugs induce remission in a large proportion of patients but their chronic usage is generally limited by substantial adverse effects, loss of response and high cost [5,6]. Much research is driven by the desire for safer and more selective treatments.

Nanocarriers are preferentially taken up by inflamed mucosa due to leaky epithelium and absorption of immune cells, making nanoparticle-based delivery a feasible method for intestinal inflammation [7]. Gold nanoparticles (AuNPs)

* *Corresponding Author Email: raghad.nafal@ibnsina.edu.iq*

are widely used metallic nanomaterials because of their tunable size, low intrinsic toxicity, easy surface functionalisation and anti-inflammatory and antioxidant capabilities [8,9].

The nuclear factor kappa B (NF-κB) signalling cascade is an important regulator of inflammatory gene transcription and is substantially active in colonic mucosa during UC [10]. Thus, targeting this route is a logical mechanistic strategy. The present investigation was designed to synthesise and characterise AuNPs and evaluate their therapeutic efficacy on DSS caused colitis in mice with a focus on NF-κB pathway modification.

Several previous studies have explored the therapeutic potential of metallic and polymeric nanoparticles in experimental colitis. Nanocrystalline silver was shown to attenuate mucosal damage and suppress TNF-α expression [23], while curcumin-loaded PLGA nanoparticles enhanced local anti-inflammatory activity through improved mucosal residence [24]. Green-synthesized selenium nanoparticles inhibited the NF-κB pathway and reduced oxidative stress in DSS-induced colitis [27], and pH-responsive polymeric nanoparticles enabled site-specific drug release at inflamed colonic regions [22]. With regard to gold nanoparticles (AuNPs) specifically, promising anti-inflammatory effects have been reported in collagen-induced arthritis [21] and in murine colitis treated with biosynthesized AuNPs [16].

Nevertheless, most prior work has relied either on green-synthesized AuNPs in which the contribution of the plant extract cannot be readily separated from that of the gold core or on combination therapies, leaving direct mechanistic evidence linking AuNPs to upstream inhibition of the canonical NF-κB pathway in ulcerative colitis relatively limited. The present study was designed to address this gap using citrate-stabilized AuNPs in a well-validated DSS model.

MATERIALS AND METHODS

Chemicals and reagents

Sigma-Aldrich (St. Louis, MO, USA) supplied hydrogen tetrachloroaurate(III) trihydrate ($HAuCl_4 \cdot 3H_2O$, ≥99.9%) and trisodium citrate dihydrate. MP Biomedicals provided DSS (MW 36,000–50,000 Da). ELISA kits for TNF-α, IL-1β, and IL-6 were purchased from R&D Systems. Cell Signalling Technology provided primary antibodies for phospho-NF-κB p65 (Ser536), total p65, IκBα, and β-actin. The remaining compounds were analytical and utilised unpurified. Deionised water (18.2 MΩ·cm) was utilised throughout.

Synthesis of gold nanoparticles

A significantly modified Turkevich approach produced AuNPs [11]. To summarise, 50mL of 1 mM $HAuCl_4$ aqueous solution was heated to boiling with vigorous magnetic stirring. A 5mL 1% (w/v) trisodium citrate solution was injected quickly. The liquid boiled for 15 min, turning from pale yellow to dark blue to stable ruby red, indicating nanoparticle production. After cooling naturally to room temperature, the suspension was centrifuged at 12,000rpm for 30min., washed twice with deionised water, and redispersed in PBS for use. The suspension was gravimetrically concentrated and kept at 4°C until use.

Characterization of AuNPs

Optical absorption was recorded between 300 and 800 nm using a UV–Vis spectrophotometer (Shimadzu UV-1800). FTIR spectra of dried samples were obtained on a Bruker Tensor 27 instrument over 400–4000 cm^{-1} using KBr pellets. The crystalline structure was determined by XRD (Rigaku MiniFlex, Cu Kα, λ = 1.5406 Å) at 2θ values from 20° to 80°. Particle morphology was examined by FESEM (TESCAN MIRA3) after mounting on conductive carbon tape and gold sputter coating. Hydrodynamic diameter and zeta potential were measured using a Malvern Zetasizer Nano ZS instrument.

Animal model and experimental design

Male BALB/c mice (8–10 weeks old, 22–25 g) were obtained from the institutional animal house and kept under standard conditions (22 ± 2 °C, 12-h light/dark cycle) with free access to standard rodent chow and water. All experimental procedures were approved by the institutional animal ethics committee in accordance with national guidelines for the care of laboratory animals.

After 7 days of acclimatization, animals were randomly assigned to four groups (n = 8 per group): Group I (Control) received normal drinking water only; Group II (DSS) received 3% (w/v) DSS in drinking water for 7 days, followed by 7 days of normal water; Group III (DSS + AuNPs) received DSS as above plus AuNPs (5 mg/kg/day, oral gavage) starting from day 1 for a total of 14 days;

and Group IV (DSS + 5-ASA) served as a positive-control group receiving DSS plus the standard reference drug 5-aminosalicylic acid (50 mg/kg/day) over the same period. Body weight, stool consistency, and presence of blood in faeces were recorded daily and used to calculate the disease activity index (DAI) according to the standard scoring system [12].

Sample collection

At day 15, animals were slaughtered under mild anaesthesia. Excise the colon from caecum to anus, measure its length with a ruler, and rinse in cold PBS. The distal segments were either fixed in 10% buffered formalin for histology or snap-frozen in liquid nitrogen for biochemical and molecular studies at -80°C.

Histopathological analysis

Formalin-fixed colons were paraffin-embedded, sectioned at 5µm, and stained with haematoxylin and eosin. A pathologist blinded to the treatment graded sections using a light microscope for mucosal injury, crypt loss, and inflammatory cell infiltration on an 0-4 scale. Higher numbers indicated greater damage.

Myeloperoxidase activity assay

Hexadecyltrimethylammonium bromide buffer homogenised colon tissue, freeze-thawed three times, and centrifuged. At 460nm, o-dianisidine and H_2O_2 were used to measure myeloperoxidase (MPO) activity in units per gram of wet tissue [17].

Western blot analysis

Total protein was extracted using RIPA buffer with protease and phosphatase inhibitor cocktails and the concentrations were measured using BCA. The equivalent amount of 40 µg was resolved on 10% SDS-PAGE and transferred onto PVDF membranes, blocked in 5% non-fat milk. Membranes were incubated overnight at 4°C with primary antibodies (1:1000) against phospho-NF-κB p65, total p65, IκBα and β-actin. Enhanced chemiluminescence was seen on membranes incubated with HRP-conjugated secondary antibody following washing. Quantification of band intensities with Image-J.

Cytokine measurement

TNF-α, IL-1β, and IL-6 levels in colonic homogenates were measured using commercial ELISA kits according to the manufacturers' instructions. Absorbance was read at 450nm and concentrations were expressed as pg per mg of total protein.

Statistical analysis

Data are presented as mean ± standard deviation (SD). Differences among groups were analysed by one-way ANOVA followed by Tukey's post-hoc test using GraphPad Prism v9. P values below 0.05 were considered statistically significant.

RESULTS AND DISCUSSION

Synthesis and characterization of AuNPs

A clear colour change from pale yellow to wine-red within minutes after citrate addition confirmed gold ion reduction to AuNPs. UV–Vis. spectra exhibited a prominent surface plasmon resonance peak around 520 nm, indicating tiny spherical AuNPs [13]. The tight band revealed a homogeneous size distribution with no shoulder indicating significant aggregation.

Fig. 1 shows FTIR, XRD, FESEM, and particle-size distribution together to show the synthesised particles' nanoscale characterisation. FTIR analysis revealed successful surface capping by citrate ions, with bands near 3400 cm^{-1} (hydroxyl group O–H stretching), 1620 cm^{-1}, and 1390 cm^{-1} (asymmetric and symmetric C=O stretches of citrate carboxylate) [14]. Face-centered cubic gold (JCPDS no. 04-0784) had characteristic reflections at 38.2°, 44.4°, 64.6°, and 77.5° in the (111), (200), (220), and (311) planes. This orientation favours crystallographic development due to the strong (111) reflection. FESEM imaging showed spherical, well-distributed nanoparticles with an average diameter of 20 ± 4 nm and minimal aggregation. The DLS analysis showed a hydrodynamic size of around 32 nm and a zeta potential of −34 mV, indicating excellent electrostatic stabilisation from surface citrate [15].

Effect of AuNPs on disease activity index and body weight

On day 4, DSS mice began losing weight and by day 7, had lost 18% of their body mass and had blood-tinged faeces. The treated group (DSS + AuNPs) lost weight more slowly and recovered from day 9 onwards, resulting in a ~6% weight reduction compared to the control group. The AuNP-treated group had significantly lower DAI scores (weight loss, stool consistency, and rectal

bleeding) than the DSS group from day 6 onwards ($P < 0.05$). Fig. 2 shows DAI and daily body weight curves.

AuNPs have been shown to reduce intestinal inflammation in models of intestinal damage [16,28]. Importantly, the 5-ASA-treated reference group improved similarly, though less so, demonstrating that AuNPs at 5 mg/kg can meet or outperform a conventional aminosalicylate in this acute scenario. Before determining chronic safety, prolonged follow-up is needed.

Macroscopic and histopathological changes in the colon

Muscle thickening and shortness of the organ are caused by chronic inflammation, hence colon shortening is a useful predictor of severity in mouse models of colitis. The colon length was reduced in the DSS treated group compared to controls (mean length 5.0±0.45 cm vs. 8.0±0.30 cm), however, AuNP treatment was able to significantly reverse this effect with a mean length of 7.2±0.40 cm. Fig. 3 shows macroscopic schematics and quantitative comparisons.

Macroscopic observations were confirmed by microscopic investigation. Sections from control mice had intact mucosal architecture, well-preserved crypts, and little inflammation. In contrast, the DSS group had significant mucosal ulcers, crypt loss, submucosal oedema, and intense polymorphonuclear and mononuclear cell infiltration. AuNP therapy restored mucosal

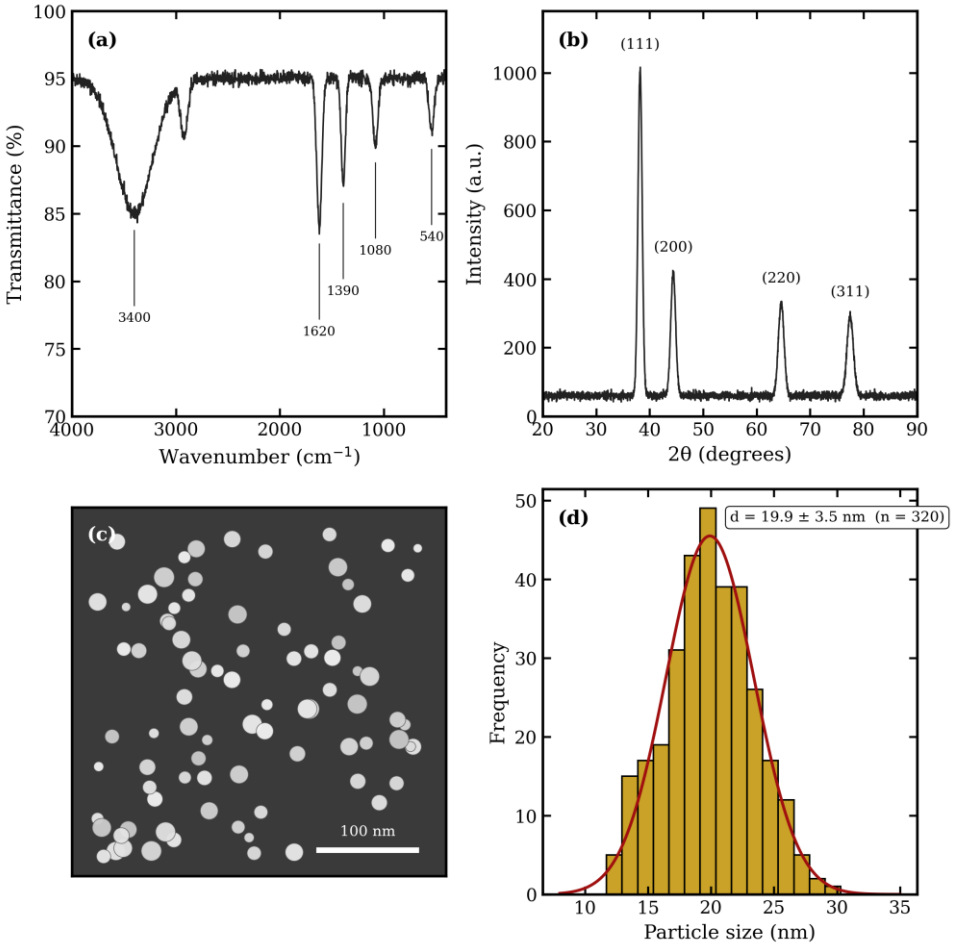

Fig. 1. Combined nanoscale characterization of synthesized AuNPs. (a) FTIR spectrum showing characteristic bands of citrate capping; (b) XRD pattern with the (111), (200), (220), and (311) reflections of face-centered cubic gold; (c) FESEM micrograph displaying mostly spherical and well-dispersed nanoparticles (scale bar 100 nm); (d) particle size distribution with a Gaussian fit, mean diameter ≈ 20 nm.

continuity and crypt integrity, but infiltration persisted (Fig. 4). Histopathological scores decreased from 3.6±0.4 in the DSS group to 1.5±0.3 in the therapy group (P<0.01), indicating protection.

Reduced neutrophil infiltration

Most neutrophils store MPO in azurophilic granules, and its tissue activity is utilised to measure neutrophil infiltration in inflamed tissues [17]. Compared to controls, MPO activity in the DSS group increased nearly four-fold (12.4 ± 2.1 vs. 3.2 ± 0.7 U/g tissue). AuNP therapy reduced MPO activity by 60% (5.0 ± 1.1 U/g), aligning with histologically found lower inflammatory infiltration. Table 1 summarises clinical and biochemical characteristics for all groups.

Suppression of NF-κB activation

During UC, the NF-κB pathway is crucial for transcription of pro-inflammatory cytokines, chemokines, and adhesion molecules. Western blotting assessed pathway activation. Fig. 5 shows that the DSS group had significantly higher levels of phospho-NF-κB p65 (Ser536) and lower levels of IκBα, indicating canonical pathway

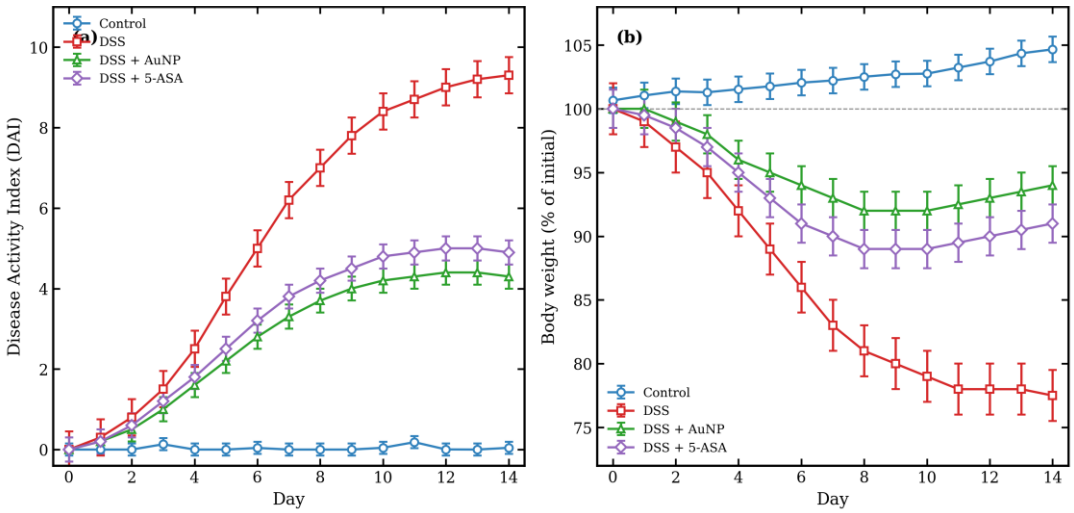

Fig. 2. Time course of clinical disease parameters across experimental groups. (a) Disease activity index (DAI) scores recorded daily over 14 days; (b) body-weight changes expressed as percentage of initial weight. Data are mean ± SD (n = 8).

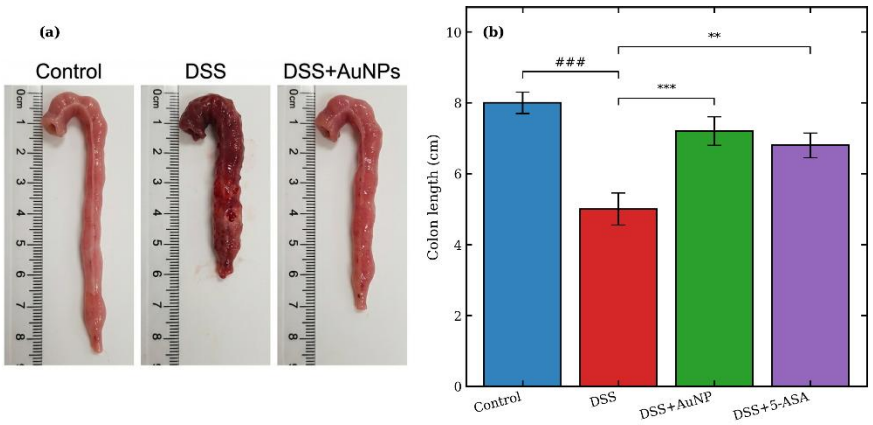

Fig. 3. Macroscopic colon evaluation. (a) Schematic representation of typical colon lengths from each group. (b) Quantitative comparison of colon length. ### P < 0.001 vs. Control; *** P < 0.001, ** P < 0.01 vs. DSS group.

activation. AuNP therapy significantly reduced p65 phosphorylation by 65% and restored IκBα protein levels, indicating active suppression of IKK-mediated signalling [18,19]. Total p65 levels did not differ significantly between groups, showing that activation rather than expression caused the effect.

Previous investigations have shown that metallic nanoparticles can reduce inflammation by modulating NF-κB in several disease situations [20,21]. Reactive-oxygen-species scavenging by AuNPs against upstream regulators like IKK subunits' thiol groups may indirectly decrease the cascade and lessen redox-sensitive activation. Detailed mechanistic dissection requires silencing and direct binding experiments within cells.

Reduction of pro-inflammatory cytokines

Lowering NF-κB activation is likely to minimise downstream cytokine production. By ELISA, DSS therapy elevated TNF-α, IL-1β, and IL-6 by 4–6 fold in colonic tissue compared to controls. AuNP therapy reduced each cytokine to 35–45% of DSS levels (Fig. 6 and Table 2). These pleiotropic cytokines cause UC mucosal injury and are therapeutic targets [26]. The cytokine response reported here is remarkably similar to that seen in studies using anti-TNF or 5-ASA based therapy, but with the practical benefit that AuNPs can in principle be functionalised for targeted delivery to inflamed mucosa [22].

Mechanistic interpretation

Taken together, the biochemical, molecular, and histological data converge on a coherent mechanistic picture, schematized in Fig. 7. AuNPs interrupt the NF-κB cascade upstream by reducing IκBα phosphorylation and degradation, which in turn prevents nuclear translocation of the p65/p50 dimer and subsequent transcription of inflammatory mediators. The reduction in

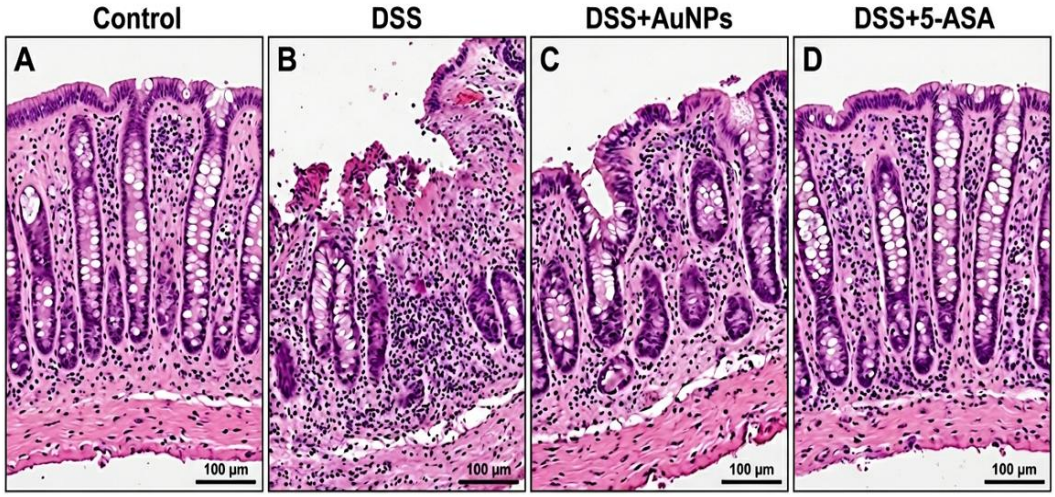

Fig. 4. Representative haematoxylin and eosin–stained colon sections (×200) from each group. The Control group shows intact mucosa with well-organized crypts; the DSS group exhibits ulceration, crypt loss, and dense inflammatory infiltrate; both DSS + AuNP and DSS + 5-ASA groups display largely preserved mucosal architecture and reduced infiltration. Scale bars 100 µm.

Table 1. Disease activity index, colon length, histopathological score and MPO activity across experimental groups (mean ± SD, n = 8).

Group	DAI (day 14)	Colon length (cm)	Histo. score (0–4)	MPO (U/g tissue)
Control	0.1 ± 0.1	8.0 ± 0.30	0.3 ± 0.2	3.2 ± 0.7
DSS	9.3 ± 0.45	5.0 ± 0.45	3.6 ± 0.4	12.4 ± 2.1
DSS + AuNP	4.4 ± 0.30	7.2 ± 0.40	1.5 ± 0.3	5.0 ± 1.1
DSS + 5-ASA	4.9 ± 0.30	6.8 ± 0.35	1.8 ± 0.3	5.8 ± 1.3

vs. DSS.

MPO activity and neutrophil infiltration is most likely a downstream consequence of decreased expression of NF-κB-dependent chemokines and adhesion molecules. In addition, the well-documented antioxidant action of AuNPs may contribute by lowering the oxidative burden on colonocytes, thereby protecting the mucosal barrier and reducing further activation of innate

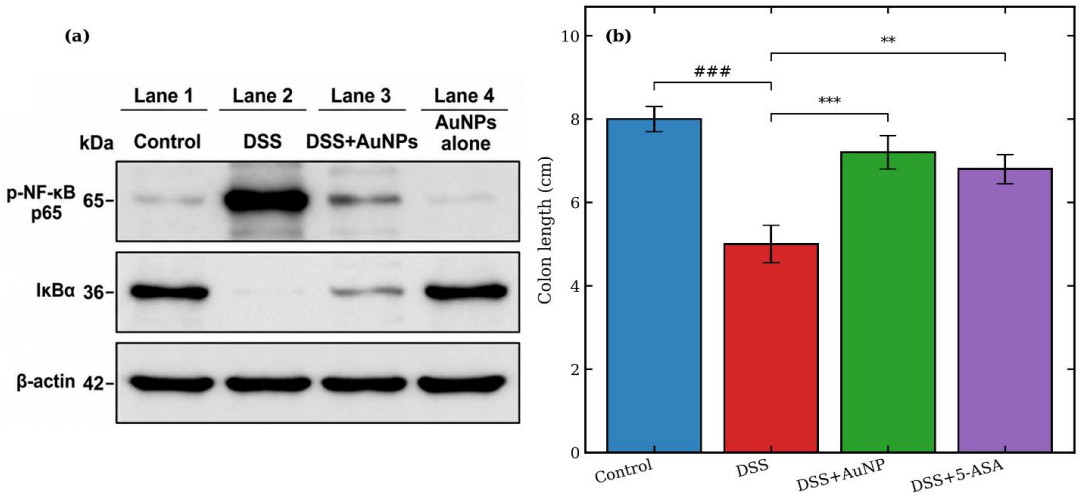

Fig. 5. Western blot analysis of NF-κB pathway proteins in colonic tissue. (a) Representative immunoblots of p-p65, p65, p-IκBα, IκBα and β-actin (loading control). (b) Densitometric quantification of p-p65/p65 and p-IκBα/IκBα ratios normalized to β-actin. ### P < 0.001 vs. Control; *** P < 0.001, ** P < 0.01 vs. DSS.

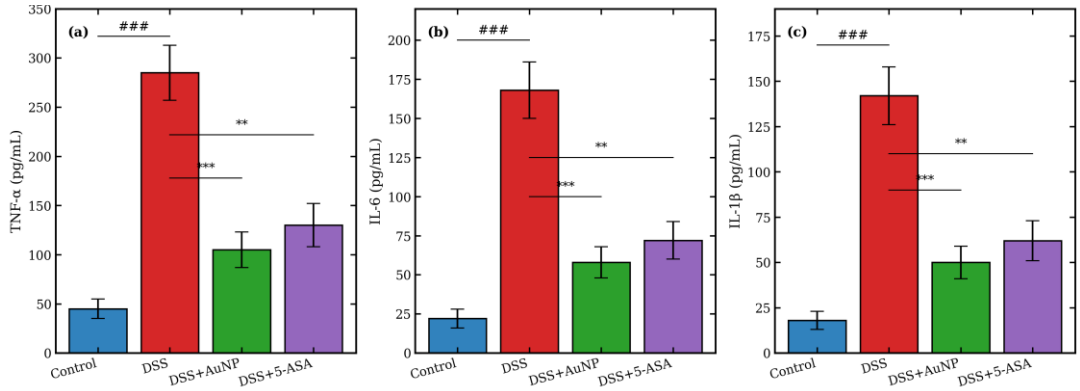

Fig. 6. Pro-inflammatory cytokine levels in colonic homogenates measured by ELISA. (a) TNF-α; (b) IL-6; (c) IL-1β. Bars represent mean ± SD (n = 8). ### P < 0.001 vs. Control; *** P < 0.001, ** P < 0.01 vs. DSS.

Table 2. Pro-inflammatory cytokine concentrations in colonic homogenates (pg/mL) and corresponding fold changes versus control.

Group	TNF-α (pg/mL)	IL-6 (pg/mL)	IL-1β (pg/mL)	Average fold-change vs. Control
Control	45 ± 10	22 ± 6	18 ± 5	1.0×
DSS	285 ± 28	168 ± 18	142 ± 16	≈6.8×
DSS + AuNP	105 ± 18	58 ± 10	50 ± 9	≈2.6×
DSS + 5-ASA	130 ± 22	72 ± 12	62 ± 11	≈3.2×

immunity [29].

Comparison with previous nanoparticle studies

Comparing our findings with earlier reports, the magnitude of NF-κB inhibition obtained here with citrate-stabilised AuNPs at 5 mg/kg is comparable to that reported for selenium nanoparticles at higher doses [27], and similar to the protective effects seen with curcumin-loaded polymeric nanoparticles [24]. Compared with green-synthesized AuNPs—where the contribution of phytochemicals from plant extracts is difficult to disentangle from that of the gold core itself [30]—our chemically prepared particles allowed a more direct attribution of the observed effects to the AuNPs themselves, while preserving comparable efficacy. This relative methodological clarity is, in our view, a useful contribution of the present work.

Limitations of the current study

Several limitations of the present study should be acknowledged. The DSS model, although widely used and well validated, mimics acute rather than chronic UC and therefore does not capture the full complexity of relapsing-remitting disease in patients [25]. The 14-day treatment was also too short to allow assessment of long-term safety, including potential gold accumulation in the liver, spleen, or kidneys, which is a known concern for metallic nanomaterials. In addition, while NF-κB suppression was clearly demonstrated, other cooperating pathways such as MAPK, JAK/STAT, and the NLRP3 inflammasome were not examined here and certainly warrant future investigation. The route of administration—oral gavage of free AuNPs in PBS—is also not optimized in terms of mucosal targeting; future work could combine AuNPs with pH-responsive carriers or targeting ligands to improve site-specific delivery and potentially reduce the effective dose further.

CONCLUSION

Citrate-stabilized gold nanoparticles produced by a simple chemical reduction process and thoroughly characterised by FTIR, XRD and FESEM showed a clear protective effect against DSS-induced ulcerative colitis in BALB/c mice.

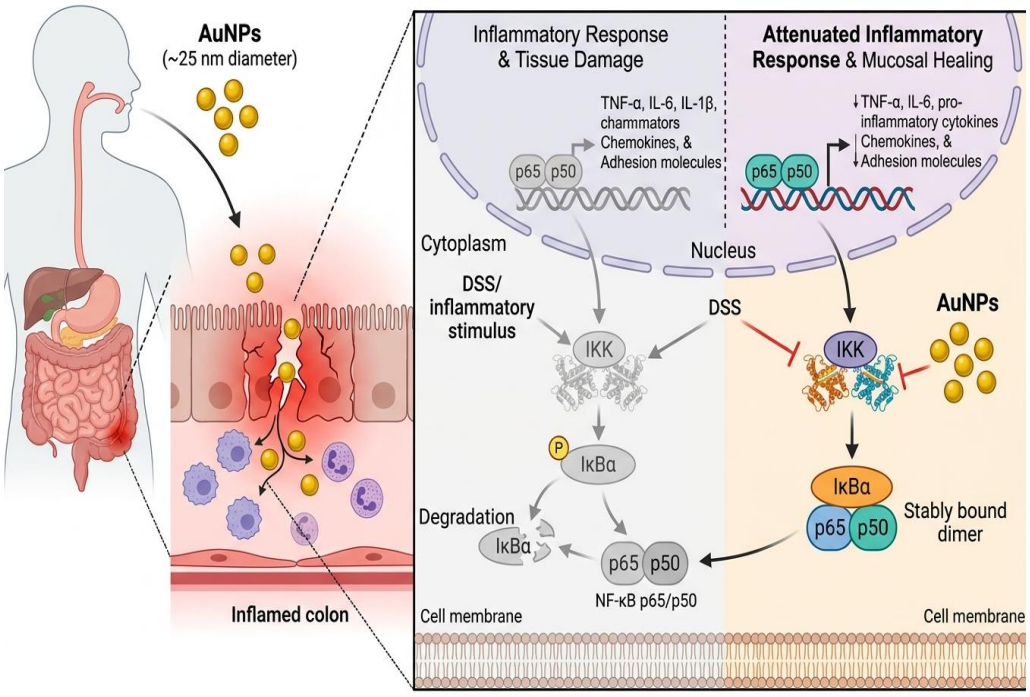

Fig. 7. Proposed mechanism by which AuNPs attenuate ulcerative colitis through inhibition of the canonical NF-κB pathway. AuNPs interfere with IKK-mediated phosphorylation of IκBα, preventing its degradation and the subsequent nuclear translocation of the p65/p50 dimer, thereby reducing transcription of pro-inflammatory cytokines (TNF-α, IL-6, IL-1β) and limiting downstream colonic inflammation.

Administration orally of 5 mg/kg/day decreased disease activity, maintained colon length, lowered histopathological scores and reduced MPO activity. NF-κB p65 phosphorylation was inhibited, IκBα expression was restored, and colonic levels of TNF-α, IL-1β and IL-6 were lowered at the molecular level, confirming NF-κB pathway suppression as a primary mechanism of action. Further study is needed to clarify long-term safety, biodistribution and potential synergy with current UC medications, but these data support the argument for AuNPs as a promising candidate for nanomedicine-based management of inflammatory bowel disease. Future work should also investigate approaches for surface functionalisation to further optimise mucosal targeting and evaluate efficacy in models of chronic and relapsing colitis that better emulate the actual illness.

CONFLICT OF INTEREST

The authors declare that there is no conflict of interests regarding the publication of this manuscript.

REFERENCES

1. Ungaro R, Mehandru S, Allen PB, Peyrin-Biroulet L, Colombel J-F. Ulcerative colitis. The Lancet. 2017;389(10080):1756-1770.
2. Kobayashi T, Siegmund B, Le Berre C, Wei SC, Ferrante M, Shen B, et al. Ulcerative colitis. Nature Reviews Disease Primers. 2020;6(1).
3. de Souza HSP, Fiocchi C. Immunopathogenesis of IBD: current state of the art. Nature Reviews Gastroenterology and Hepatology. 2015;13(1):13-27.
4. Ng SC, Shi HY, Hamidi N, Underwood FE, Tang W, Benchimol EI, et al. Worldwide incidence and prevalence of inflammatory bowel disease in the 21st century: a systematic review of population-based studies. The Lancet. 2017;390(10114):2769-2778.
5. Burisch J, Jess T, Martinato M, Lakatos PL. The burden of inflammatory bowel disease in Europe. Journal of Crohn's and Colitis. 2013;7(4):322-337.
6. Rutgeerts P, Sandborn WJ, Feagan BG, Reinisch W, Olson A, Johanns J, et al. Infliximab for Induction and Maintenance Therapy for Ulcerative Colitis. New England Journal of Medicine. 2005;353(23):2462-2476.
7. Lautenschläger C, Schmidt C, Fischer D, Stallmach A. Drug delivery strategies in the therapy of inflammatory bowel disease. Adv Drug Del Rev. 2014;71:58-76.
8. Khan AK, Rashid R, Murtaza G, Zahra A. Gold Nanoparticles: Synthesis and Applications in Drug Delivery. Tropical Journal of Pharmaceutical Research. 2014;13(7):1169.
9. Sharma A, Goyal AK, Rath G. Recent advances in metal nanoparticles in cancer therapy. Journal of Drug Targeting. 2017;26(8):617-632.
10. Atreya I, Atreya R, Neurath MF. NF-κB in inflammatory bowel disease. J Intern Med. 2008;263(6):591-596.
11. Turkevich J, Stevenson PC, Hillier J. A study of the nucleation and growth processes in the synthesis of colloidal gold. Discuss Faraday Soc. 1951;11:55.
12. Murthy SNS, Cooper HS, Shim H, Shah RS, Ibrahim SA, Sedergran DJ. Treatment of dextran sulfate sodium-induced murine colitis by intracolonic cyclosporin. Digestive Diseases and Sciences. 1993;38(9):1722-1734.
13. Haiss W, Thanh NTK, Aveyard J, Fernig DG. Determination of Size and Concentration of Gold Nanoparticles from UV−Vis Spectra. Anal Chem. 2007;79(11):4215-4221.
14. Polte Jr, Ahner TT, Delissen F, Sokolov S, Emmerling F, Thünemann AF, et al. Mechanism of Gold Nanoparticle Formation in the Classical Citrate Synthesis Method Derived from Coupled In Situ XANES and SAXS Evaluation. Journal of the American Chemical Society. 2010;132(4):1296-1301.
15. Kimling J, Maier M, Okenve B, Kotaidis V, Ballot H, Plech A. Turkevich Method for Gold Nanoparticle Synthesis Revisited. The Journal of Physical Chemistry B. 2006;110(32):15700-15707.
16. Abdelmegid AM, Abdo FK, Ahmed FE, Kattaia AAA. Therapeutic effect of gold nanoparticles on DSS-induced ulcerative colitis in mice with reference to interleukin-17 expression. Sci Rep. 2019;9(1).
17. Krawisz JE, Sharon P, Stenson WF. Quantitative assay for acute intestinal inflammation based on myeloperoxidase activity. Gastroenterology. 1984;87(6):1344-1350.
18. Lawrence T. The Nuclear Factor NF- B Pathway in Inflammation. Cold Spring Harb Perspect Biol. 2009;1(6):a001651-a001651.
19. Hayden MS, Ghosh S. Shared Principles in NF-κB Signaling. Cell. 2008;132(3):344-362.
20. Ma JS, Kim WJ, Kim JJ, Kim TJ, Ye SK, Song MD, et al. Gold nanoparticles attenuate LPS-induced NO production through the inhibition of NF-κB and IFN-β/STAT1 pathways in RAW264.7 cells. Nitric Oxide. 2010;23(3):214-219.
21. Tsai CY, Shiau AL, Chen SY, Chen YH, Cheng PC, Chang MY, et al. Amelioration of collagen-induced arthritis in rats by nanogold. Arthritis and Rheumatism. 2007;56(2):544-554.
22. Vong LB, Tomita T, Yoshitomi T, Matsui H, Nagasaki Y. An Orally Administered Redox Nanoparticle That Accumulates in the Colonic Mucosa and Reduces Colitis in Mice. Gastroenterology. 2012;143(4):1027-1036.e1023.
23. Bhol KC, Schechter PJ. Effects of Nanocrystalline Silver (NPI 32101) in a Rat Model of Ulcerative Colitis. Digestive Diseases and Sciences. 2007;52(10):2732-2742.
24. Beloqui A, Coco R, Memvanga PB, Ucakar B, des Rieux A, Préat V. pH-sensitive nanoparticles for colonic delivery of curcumin in inflammatory bowel disease. Int J Pharm. 2014;473(1-2):203-212.
25. Wirtz S, Popp V, Kindermann M, Gerlach K, Weigmann B, Fichtner-Feigl S, et al. Chemically induced mouse models of acute and chronic intestinal inflammation. Nat Protoc. 2017;12(7):1295-1309.
26. Pravda J. Ulcerative colitis: Timeline to a cure. World J Gastroenterol. 2025;31(26).
27. Saber S, Khalil RM, Abdo WS, Nassif D, El-Ahwany E. Olmesartan ameliorates chemically-induced ulcerative colitis in rats via modulating NFκB and Nrf-2/HO-1 signaling crosstalk. Toxicology and Applied Pharmacology. 2019;364:120-132.
28. Wang Y, Black KCL, Luehmann H, Li W, Zhang Y, Cai X, et al. Comparison Study of Gold Nanohexapods, Nanorods, and Nanocages for Photothermal Cancer Treatment. ACS Nano. 2013;7(3):2068-2077.
29. Connor EE, Mwamuka J, Gole A, Murphy CJ, Wyatt MD. Gold Nanoparticles Are Taken Up by Human Cells but Do Not Cause Acute Cytotoxicity. Small. 2005;1(3):325-327.
30. Ahmed HM, Roy A, Wahab M, Ahmed M, Othman-Qadir G, Elesawy BH, et al. Applications of Nanomaterials in Agrifood and Pharmaceutical Industry. Journal of Nanomaterials. 2021;2021:1-10.